Fermi-surface topology and the effects of intrinsic disorder in a class of charge-transfer salts containing magnetic ions: β''-(BEDT-TTF)$_4$[$(H_3O)M(C_2O_4)_3$]Y (M=Ga, Cr, Fe; Y=C_5H_5N)

A. I. Coldea and A. F. Bangura
Clarendon Laboratory, University of Oxford, Parks Road, Oxford OX1 3PU, United Kingdom

J. Singleton
National High Magnetic Field Laboratory, Los Alamos National Laboratory, TA-35, MS-E536, Los Alamos, New Mexico 87545, USA

A. Ardavan
Clarendon Laboratory, University of Oxford, Parks Road, Oxford OX1 3PU, United Kingdom

A. Akutsu-Sato,* H. Akutsu,† S. S. Turner, and P. Day
Davy-Faraday Research Laboratory, The Royal Institution, 21 Albemarle Street, London W1S 4BS, United Kingdom
(Received 7 July 2003; published 27 February 2004)

We report high-field magnetotransport measurements on β''-(BEDT-TTF)$_4$[$(H_3O)M(C_2O_4)_3$]Y, where M = Ga, Cr, and Fe and Y=C_5H_5N. We observe similar Shubnikov–de Haas oscillations in all compounds, attributable to four quasi-two-dimensional Fermi-surface pockets, the largest of which corresponds to a cross-sectional area ≈8.5% of the Brillouin zone. The cross-sectional areas of the pockets are in agreement with the expectations for a compensated semimetal, and the corresponding effective masses are $\sim m_e$, rather small compared to those of other BEDT-TTF salts. Apart from the case of the smallest Fermi-surface pocket, varying the M ion seems to have little effect on the overall Fermi-surface topology or on the effective masses. Despite the fact that all samples show quantum oscillations at low temperatures, indicative of Fermi liquid behavior, the sample and temperature dependence of the interlayer resistivity suggest that these systems are intrinsically inhomogeneous. It is thought that intrinsic tendency to disorder in the anions and/or the ethylene groups of the BEDT-TTF molecules leads to the coexistence of insulating and metallic states at low temperatures. A notional phase diagram is given for the general family of β''-(BEDT-TTF)$_4$[$(H_3O)M(C_2O_4)_3$]Y salts.

DOI: 10.1103/PhysRevB.69.085112 PACS number(s): 71.18.+y, 71.20.Rv, 72.15.Gd, 74.10.+v

I. INTRODUCTION

Superconducting charge-transfer salts of the molecule BEDT-TTF have attracted considerable experimental and theoretical interest because of their complex pressure-temperature (P,T) phase diagrams, some of which are superficially similar to those of the ''high-T_c'' cuprate superconductors.[1–3] For example, the superconducting phase in the κ-(BEDT-TTF)$_2X$ salts is in close proximity to an antiferromagnetic insulator[4–6] and/or Mott insulator;[7] it is also surrounded by other unusual states,[4,5] including what has been termed a ''bad metal.''[7] Recent magnetization,[8] thermal expansion,[9] and resistivity[10] experiments suggest that this ''bad metal'' may in fact represent the *coexistence* of Fermi-liquid-like and insulating phases. The presence of both metallic and insulating states at low temperatures is probably related to progressive freezing-in of disorder associated with the terminal ethylene-groups of BEDT-TTF (which can adopt either a ''staggered'' or ''eclipsed'' configuration) and/or with the anions, X.[11–15] As yet there is no strong theoretical concurrence on the mechanism for superconductivity in the BEDT-TTF salts,[3,16] with electron-electron interactions, spin fluctuations,[17] charge fluctuations,[18] and electron-phonon interactions[19] under consideration. It is therefore unclear as to whether the mixed insulating/metallic phase referred to above is a prerequisite for or a hindrance to superconductivity. However, a recent paper has pointed out the sensitivity of the superconductivity in BEDT-TTF salts to nonmagnetic impurities and disorder, suggesting that this is evidence for d-wave superconductivity.[20]

In order to address some of these issues we have studied a new family of charge-transfer salts of the form β''-(BEDT-TTF)$_4$[$(H_3O)M(C_2O_4)_3$]Y, where M is a magnetic [Cr^{3+} (S=3/2), Fe^{3+} (S=5/2)] or nonmagnetic [Ga^{3+} (S=0)] ion and Y is a solvent molecule such as C_5H_5N (pyridine), C_6H_5CN (benzonitrile) or $C_6H_5NO_2$ (nitrobenzene). Y essentially acts as a template molecule, helping to stabilize the structure; its size and electronegativity affect the unit cell volume, and the amount of disorder in the system.[21–26] The unit-cell volume is also affected by changing the M ion inside the tris(oxalate) structure.[22,23,25,26] Furthermore, a subsidiary motive for varying M is to search for potential role for magnetism in the mechanism for superconductivity.[21] In this context, the magnetic charge-transfer salt λ-(BETS)$_2$FeCl$_4$ (Refs. 27,28) has been found to exhibit a field-induced superconducting state in fields ≳17 T. Whilst these data appear to be explicable by the Jaccarino-Peter compensation effect,[27,29,30] others have suggested that the Fe ions play some role in the superconducting state.[28,31] Although there are many detailed differences between individual samples, the β''-(BEDT-TTF)$_4$[$(H_3O)M(C_2O_4)_3$]Y salts show two distinct classes of low-temperature behavior, superconducting and metallic as summarized in Fig. 1, which shows the interlayer magnetoresistivity ρ_{zz} (see Sec. II) of three samples at a temperature T=0.50 K. Salts with Y=C_6H_5CN (benzoni-

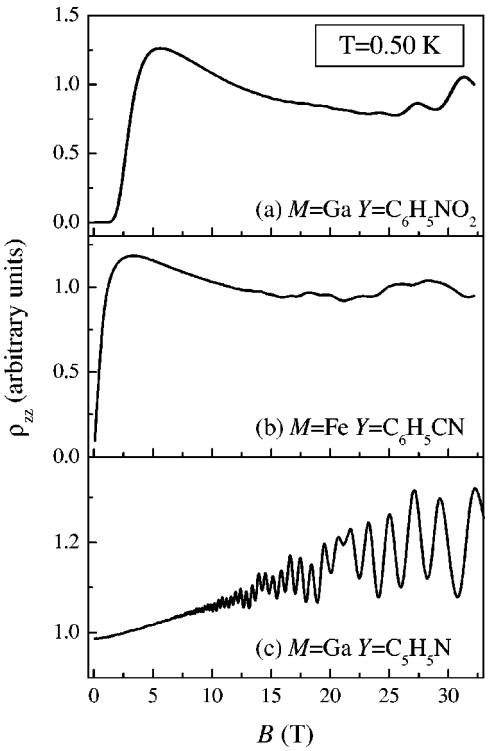

FIG. 1. Magnetic-field dependence of the interplane resistivity, ρ_{zz} for β''-(BEDT-TTF)$_4$[$(H_3O)M(C_2O_4)_3$]Y samples containing different Y molecules and transition metal ions M. Data are shifted vertically for clarity. Salts with (a) $Y=C_6H_5NO_2$ or (b) $Y=C_6H_5CN$ typically exhibit superconductivity, negative magnetoresistance and a simple set of Shubnikov–de Haas oscillations. By contrast, the (c) $Y=C_5H_5N$ (pyridine) salt shows no superconductivity, positive magnetoresistance and a complex series of Shubnikov–de Haas oscillations; this is entirely typical of the salts containing pyridine.

trile) or $C_6H_5NO_2$ (nitrobenzene) are superconductors.[21,24] At temperatures below the superconducting-to-normal transition, they tend to exhibit negative magnetoresistance, on which is superimposed one or two series of Shubnikov–de Haas oscillations of relatively low frequency.[24] On the other hand, salts with $Y=C_5H_5N$ are not superconducting; they exhibit positive magnetoresistance, and display a complex mixture of higher-frequency Shubnikov–de Haas oscillations. In this paper we shall concentrate on the $Y=C_5H_5N$ salts, deriving their Fermi-surface parameters and quasiparticle scattering rates whereas the superconductors with $Y=C_6H_5CN$ or $C_6H_5NO_2$ are described in detail in another paper.[24] However, in deriving a general phase diagram (Sec. V) we shall discuss the latter superconducting materials in general terms alongside the $Y=C_5H_5N$ salts.

This paper is organized as follows. Experimental details are given in Sec. II whereas the relevant structural details and the behavior of the β''-(BEDT-TTF)$_4$[$(H_3O)M(C_2O_4)_3$]C_5H_5N samples on cooling from room to cryogenic temperatures are given in Sec. III, which also outlines the mechanisms which introduce disorder. Magnetoresistance data analyzed in Sec. IV shows the Shubnikov–de Haas oscillations which suggest that there are four Fermi-surface pockets, the areas

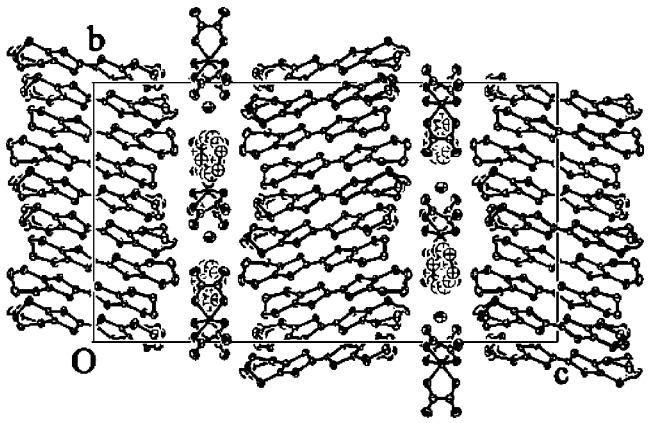

FIG. 2. Monoclinic crystal structure of β''-(BEDT-TTF)$_4$[$(H_3O)M(C_2O_4)_3$]C_5H_5N projected along the a axis (Ref. 22).

of which obey the additive relationship expected for a compensated semimetal. The results are discussed in Sec. V and a notional phase diagram for the β''-(BEDT-TTF)$_4$[$(H_3O)M(C_2O_4)_3$]Y salts is proposed showing the influence of unit cell size and disorder. A summary is given in Sec. VI.

II. EXPERIMENTAL DETAILS

The β''-(BEDT-TTF)$_4$[$(H_3O)M(C_2O_4)_3$]Y samples were grown using electrocrystallization techniques as described elsewhere;[21–23] they are generally $\sim 1\times1\times0.2$ mm^3 hexagonal platelets or needles. It is possible to deduce the upper and lower faces that are parallel to the highly conducting quasi-two-dimensional planes by visual inspection. Electrical contacts were made to these surfaces by using graphite paint to attach 12 μm platinum wires. The interlayer (magneto)resistance $R_{zz} \propto \rho_{zz}$ (Ref. 3) was measured using standard four-terminal ac techniques. This involves driving the current and measuring the voltage between pairs of contacts on the upper and lower surfaces.[3] Magnetoresistance experiments were carried out in quasistatic fields provided by a superconductive magnet in Oxford and a 33 T Bitter coil at NHMFL Tallahassee. The crystals were mounted in a ^{3}He cryostat which allowed rotation to all possible orientations in magnetic field; sample orientation is defined by the angle θ between the direction of the magnetic field and the normal to the quasi-two-dimensional planes and the azimuthal angle ϕ. Sample currents between 1 and 25 μA were used at typical frequencies 18–300 Hz. Although around 20 crystals have been studied, in this paper we shall focus on two or three typical samples of each salt; samples are distinguished by the consistent use of a label (e.g., $M=$Cr, sample A).

III. STRUCTURAL CONSIDERATIONS AND DISORDER IN THE LOW-TEMPERATURE PHASE

A. Structure and bandfilling

Figure 2 shows a projection of the crystal structure along the a axis of the β''-(BEDT-

TABLE I. Lattice parameters of β''-(BEDT-TTF)$_4$[$(H_3O)M(C_2O_4)_3$]Y salts ($C2/c$ symmetry group) measured around 120 K.

M/Y	a(Å)	b(Å)	c(Å)	β	V(Å^3)	T(K)	Ref.
Ga/$C_6H_5NO_2$	10.278	19.873	35.043	93.423	7145.2	100	22
Cr/$C_6H_5NO_2$	10.283	19.917	34.939	93.299	7144.4	150	26
Fe/$C_6H_5NO_2$	10.273	19.949	35.030	92.969	7169.6	120	26
Cr/C_6H_5CN	10.240	19.965	34.905	93.69	7121.6	120	25
Fe/C_6H_5CN	10.232	20.043	34.972	93.25	7157	120	21
Ga/C_5H_5N	10.258	19.701	34.951	93.366	7051.9	120	22
Fe/C_5H_5N	10.267	19.845	34.907	93.223	7101.0	150	23

TTF)$_4$[$(H_3O)M(C_2O_4)_3$]C_5H_5N salts, and Table I gives the lattice parameters (around 120 K) for all compounds studied in this paper and in Ref. 24. The structure consists of alternating BEDT-TTF and anion layers, the latter containing the metal tris(oxalate) $[M(C_2O_4)_3]^{3-}$, the ion H_3O^+ and the solvent molecule, Y. The molecules in the anion layer lie in a ''honeycomb'' arrangement with alternate H_3O^+ and metal oxalates giving an approximately hexagonal network of cavities in which the solvent molecule Y lies. The solvent molecule helps to stabilize the structure; the plane of phenyl ring makes an angle of ≈ 32–$36°$ to the plane of the oxalate layer.[23,25,26] The metal ion M is octahedrally co-ordinated to the oxalate ligands and the oxygen atoms on the oxalates are weakly bonded to the hydrogen atoms on the terminal ethylene groups of the BEDT-TTF molecules, acting to pull these together. The BEDT-TTF molecules adopt the β'' packing arrangement in the ab planes, in which they form roughly orthogonal stacks. The crystallographic structure of our compounds is monoclinic (see Table I) with the (ab) conducting planes at a distance of $d=c/2$ from each other, as shown in Fig. 2.[23]

By far the shortest S-S distances are within the cation planes, leading to a predominantly two-dimensional band structure.[21,32] Each BEDT-TTF molecule is expected to donate half an electron, leaving two holes per unit cell. Band structure calculations based on the room temperature crystallographic data suggest these salts should be compensated semimetals, with a Fermi surface consisting of quasi-two-dimensional electron and hole pockets of approximately equal area.[32] Although BEDT-TTF salts and their relatives are frequently compensated semimetals,[3] the electronlike Fermi-surface component is often a pair of open sheets; a closed electron pocket is relatively unusual, but it was found in β''-(BEDO-TTF)$_2$ReO$_4$H$_2$O.[33]

The interlayer transfer integrals will be less straightforward to calculate in the β''-(BEDT-TTF)$_4$[$(H_3O)M(C_2O_4)_3$]Y salts; the planes of the BEDT-TTF molecules in adjacent layers (as well as those of the anion layers) are twisted with respect to each other by $62 \pm 2°$, an unusual feature in BEDT-TTF salts.[21,25]

B. Disorder mechanisms

The β''-(BEDT-TTF)$_4$[$(H_3O)M(C_2O_4)_3$]Y salts are prone to structural disorder primarily because the terminal ethylene groups ($-CH_2CH_2-$) of the BEDT-TTF molecules are able to adopt different configurations (twisted/staggered or eclipsed) depending on how they interact with the anion layer.[22,23] Moreover, since C_5H_5N is smaller than the other templating Y molecules, it does not fill the whole of the hexagonal cavity. Changing the solvent molecule from $Y=C_6H_5NO_2$ to $Y=C_5H_5N$ induces additional structural freedom, leading to disorder in around one quarter of the terminal ethylene groups.[22,23] As a result, the ethylene groups are the dominant cause of both static and dynamic disorder at high temperatures, and static disorder below 90 K, the temperature around which the two different configurations are ''frozen in,''[22] as found in the κ-phase salts.[11–13]

The C_5H_5N molecule can also introduce disorder by adopting two different orientations in the anion layer. By contrast, the other solvents, $Y=C_6H_5NO_2$ and $Y=C_6H_5CN$, lock into one ordered configuration.[22]

Having discussed the various mechanisms for disorder, we shall now examine how disorder is manifested in the resistivity of the samples.

C. The temperature dependence of the resistivity

The temperature dependence of the normalized interplane resistance, $R_{zz}(T)/R_{zz}(286\ \mathrm{K})$, for five typical β''-(BEDT-TTF)$_4$[$(H_3O)M(C_2O_4)_3$]C_5H_5N samples is shown in Fig. 3; for comparison, equivalent data for $M=$Ga, $Y=C_6H_5NO_2$ are displayed in the inset. Whilst many of the features in the data are quite sample or cooling-rate dependent, all of the samples ($M=$Ga, Cr, Fe) are consistent in displaying a transition from metallic-type behavior (positive dR_{zz}/dT) to insulating-type behavior (negative dR_{zz}/dT) at $T_{\mathrm{MI}} \approx 150$ K. Values of T_{MI} are listed in Table II.

The minimum in resistance at T_{MI} may represent the onset of a possible form of density-wave state. Quasi-two-dimensional conductors in which the Fermi surface is completely gapped by a density wave exhibit a resistivity that rises by several orders of magnitude as the temperature falls, as found for (BEDT-TTF)$_3$Cl$_2$2H$_2$O (Ref. 34). By contrast, the resistance of the β''-(BEDT-TTF)$_4$[$(H_3O)M(C_2O_4)_3$]C_5H_5N salts (shown in Fig. 3) only increases by a factor of ~ 1.5–3. The latter behavior is similar to that of quasi-two-dimensional conductors in which a density wave only partially nests the Fermi surface, leaving behind residual Fermi-surface pockets as found for the Mo bronzes[35] and α-(BEDT-TTF)$_2$KHg(SCN)$_4$.[36] In such

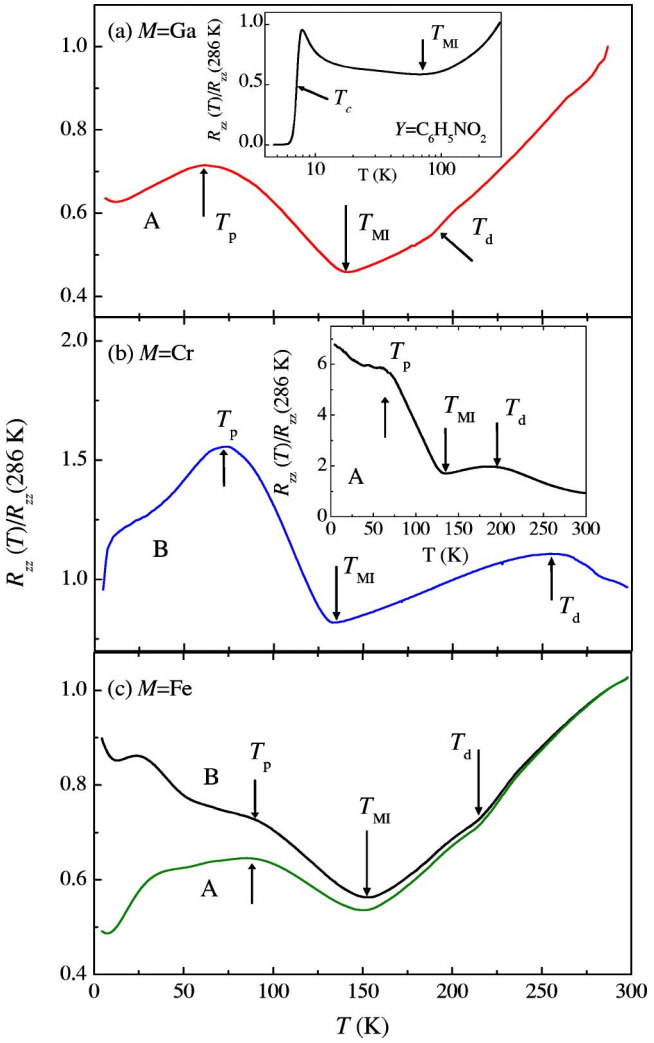

FIG. 3. Temperature dependence of the normalized interplane resistance $R_{zz}(T)/R_{zz}(286\ \mathrm{K})$ in zero magnetic field for different samples of β''-(BEDT-TTF)$_4$[$(H_3O)M(C_2O_4)_3$]C_5H_5N with (a) M=Ga (sample A) (the inset shows β''-(BEDT-TTF)$_4$[$(H_3O)M(C_2O_4)_3$]Y with M=Ga, Y=$C_6H_5NO_2$ for comparison), (b) M=Cr (sample B) [the inset shows M=Cr (sample A)] and (c) M=Fe (samples A and B). The arrows indicate the temperatures described in the text.

cases, the conductivity is a convolution of a metallic component, typically varying as a power law in temperature (due to the unnested portions of the Fermi surface) and an insulating component with an activated temperature dependence (due to the energy gap of the density-wave state).[35] The exact form of the resistivity depends on which component dominates. An alternative scenario that could potentially lead to similar resistivity behavior is the segregation of the sample into insulating and metallic domains,[37] as also proposed for the κ-(BEDT-TTF)$_2X$ salts (see Ref. 9 and references therein). In Sec. IV we shall see that the Fermi-surface topology is more complicated than that predicted by the band structure calculations, which may be additional evidence that the transition at T_{MI} is associated with the formation of a density wave.

All of the Y=C_5H_5N crystals also consistently exhibit a feature at a lower temperature, $T_p \approx 60$–80 K (shown in Fig. 3). However, depending on the sample, this is manifested either as a change from insulating- to metallic-type behavior (M=Ga, all samples; M=Cr, sample B; M=Fe sample A), or as merely a shoulder on a resistivity that continues to increase with decreasing temperature (M=Cr, sample A; M=Fe, sample B). Such a feature is also indicative of a number of contributions to the conductivity acting in parallel. For example, it is possible to reproduce the behavior of M=Cr, sample B between 60 K and T_{MI} using a resistor network model that combines metallic (resistivity $\propto T^n$, with $n \sim 1$–2) and thermally-activated components $\propto \exp(E_A/k_BT)$ (see also Ref. 38). Although the exact values obtained depend on the details of the resistor network model used, the values of E_A obtained from fitting data between T_p and T_{MI} showed a consistent increase from M=Fe ($E_A \approx 170$–220 K) through M=Ga ($E_A \approx 300$ K) to M=Cr ($E_A \approx 400$–500 K), i.e., the activation energy E_A increases with decreasing unit cell volume (see Table I).

The features discussed thus far do not seem to depend on sample cooling rate. By contrast, in all five M=Cr samples studied, there is an additional peak in the resistivity at $T_d \approx 200$–270 K, the appearance and temperature of which both depend on the sample cooling rate. By contrast, samples with M=Ga, Fe only exhibit a small inflection at T_d. At the lowest temperatures, $R_{zz}(T)/R_{zz}(286\ \mathrm{K})$ values ranging from around 0.5 (M=Fe, sample A) to 7 (M=Cr, sample A) are obtained (Fig. 3); the actual value reached seems more dependent on the sample batch rather than the identity of the M ion (e.g., compare M=Cr, samples A and B). This points to a prominent role for disorder in determining the low-temperature resistive behavior of the β''-(BEDT-TTF)$_4$[$(H_3O)M(C_2O_4)_3$]C_5H_5N salts.

As T tends to zero, the resistivity of M=Cr sample B drops quite sharply, although zero resistance is never attained. A similar drop in resistance for M=Ga below 2 K, which was destroyed by an applied field of 0.16 T, was previously reported as evidence for superconductivity.[22] However, none of the M=Ga samples studied in the present work exhibited such a feature. This is possibly related to the recent observation that superconductivity in the BEDT-TTF salts is very sensitive to disorder and nonmagnetic impurities.[20]

On the other hand, a robust superconducting state is stabilized below T_c=7 K for M=Ga and Y=$C_6H_5NO_2$ [as shown in the inset of Fig. 3(a)] and for M=Fe and Y=C_6H_5CN [Fig. 1(b) and Ref. 21]. For completeness, note that both of the latter superconducting salts show a single metal-insulator transition [see inset of Fig. 3(a)] similar to that observed at T_{MI} in the Y=C_5H_5N salts. However, for the superconducting salts T_{MI} seems somewhat sample dependent; values ranging from T_{MI}=68 K (Ref. 24) to $T_{MI} \approx 160$–180 K (Ref. 22) have been reported for the M=Ga, Y=$C_6H_5NO_2$ salt.

To summarize this section, the resistivities of the β''-(BEDT-TTF)$_4$[$(H_3O)M(C_2O_4)_3$]C_5H_5N salts exhibit a complex temperature and sample dependence (Fig. 3). The minimum in R_{zz} at T_{MI} is an intrinsic feature of all samples,

TABLE II. Parameters associated with the band structure of β''-(BEDT-TTF)$_4$[$(H_3O)M(C_2O_4)_3$]C_5H_5N for magnetic fields perpendicular to the highly conducting quasi-two-dimensional planes. Values for several samples with different M are given. The F are Shubnikov–de Haas frequencies, the subscripts α, etc. identifying the associated Fermi-surface pocket; the m^* are corresponding effective masses. $T_{D\delta}$ is the Dingle temperature for F_δ, and T_{MI} is the metal-insulator transition temperature identified in Fig. 3.

Parameters	M=Ga(A)	M=Ga(B)	M=Ga(C)	M=Cr(A)	M=Cr(B)	M=Cr (L)	M=Fe(A)	M=Fe(B)
F_α (T)	48	50	49	39	38	40	45	45
F_β (T)	89	85	92	95	95	98	94	92
F' (T)	205			190	190	195		
F'' (T)	247	240	235			243	243	
F_γ (T)	292	296	297	296	286	305	307	305
F_δ (T)	344	345	346	344	343	357	346	344
$m^*_\alpha(m_e)$		1.9±0.3	1.3±0.2	0.56±0.05	0.54±0.05	0.5±0.1	0.8±0.1	0.6±0.1
$m^*_\beta(m_e)$	0.56±0.05	0.51±0.05	0.62±0.05	0.63±0.05	0.62±0.05		0.68±0.05	0.76±0.05
$m^*_\gamma(m_e)$	0.7±0.1	1.01±0.05	1.09±0.05					
$m^*_\delta(m_e)$	0.98±0.05	0.95±0.05	0.93±0.05	1.04±0.05	0.98±0.05	0.9±0.1	0.9±0.1	1.1±0.1
$T_{D\delta}$ (K)	2.7±0.1	2.3±0.2	1.7±0.2	1.8±0.1	1.4±0.2	2.5±0.5	4±0.5	4.2±0.1
T_{MI} (K)	138±2			142±1		120±20	150±2	153±2

and, by analogy with resistivity data from other quasi-two-dimensional systems, probably indicates the onset of a density-wave state. The form of the resistivity at temperatures just below this (including the peak at T_p) suggests metallic and thermally-activated contributions to the conductivity acting in parallel. At lower temperatures, the behavior of the samples is much more divergent, with $R_{zz}(T)/R_{zz}$(286 K) values spread between 0.5 and 7 indicating an additional thermally-activated process (or processes) which is (are) probably dependent on the degree of disorder within the samples. By contrast, the temperature-dependent resistivity is rather simpler for the β''-(BEDT-TTF)$_4$[$(H_3O)M(C_2O_4)_3$]Y salts with $Y=C_6H_5NO_2$ and $Y=C_6H_5CN$. The difference may be attributable to the higher degree of structural disorder possible in the $Y=C_5H_5N$ salts, resulting from the less constrained ethylene groups and greater rotational freedom of the Y molecule.[22] Similar electronic properties determined by the disordered anions (that lock into two different configurations) were found for β''-(BEDT-TTF)$_2SF_2CHFCF_2SO_3$,[39] for which resistivity shows a metal-insulating transition near 190 K, compared with the superconducting compound, β''-(BEDT-TTF)$_2SF_2CF_2CF_2SO_3$ ($T_c=5.4$ K), which has ordered anions.[40]

IV. LOW-TEMPERATURE MAGNETORESISTANCE

A. Shubnikov–de Haas frequencies and Fermi-surface pockets

Figure 4 shows the field dependence of R_{zz} for several samples of β''-(BEDT-TTF)$_4$[$(H_3O)M(C_2O_4)_3$]C_5H_5N with M=Ga, Cr, and Fe measured at several temperatures between 0.50 K and 4.2 K. All samples exhibit Shubnikov–de Haas oscillations superimposed on a positive background magnetoresistance. Several frequencies are visible in varying proportions. For example, the dominant series of oscillations for M=Cr is of relatively low frequency, whereas the dominant oscillations for M=Ga, Fe are of a higher frequency. The amplitude of the oscillations varies slowly with temperature, suggesting the corresponding effective masses are not very large.[41]

No clear signature of superconductivity was observed either in the field, angle or temperature dependence of R_{zz} for β''-(BEDT-TTF)$_4$[$(H_3O)M(C_2O_4)_3$]Y salts when $Y=C_5H_5N$, in contrast to the case in which $Y=C_6H_5NO_2$ and $Y=C_6H_5CN_2$ [as shown in Fig. 1 and inset of Fig. 3(a)].

In order to analyze the Shubnikov–de Haas oscillations, we define the oscillatory fraction of the magnetoresistance,

$$\frac{\Delta R_{zz}}{R_{zz}}=\frac{R_{zz}-R_{bg}}{R_{zz}}. \quad (1)$$

Here R_{bg} is the slowly-varying background magnetoresistance approximated by a polynomial in B. As long as $\Delta R_{zz}/R_{zz}\ll 1$, $\Delta R_{zz}/R_{zz}\approx-\Delta\sigma_{zz}/\sigma_{bg}$, where the σ are equivalent terms in the conductivity[41,42] [$\Delta\sigma_{zz}/\sigma_{bg}$ is the quantity dealt with in the Lifshitz-Kosevich (LK) treatment of Shubnikov–de Haas oscillations[41] used to extract effective masses and the scattering time of the quasiparticles]. The $\Delta R_{zz}/R_{zz}$ values were processed using both the maximum entropy method (MEM) (filter size=200) (Ref. 43) and the fast Fourier transform (FFT) usually over the field range 7–32 T. The two methods give similar representations of the frequencies present, as shown in the right panel of Fig. 4.

We identify four frequencies which occur consistently in all of the transforms over the complete temperature range (see Figs. 4 and 5), and are similar in all β''-(BEDT-TTF)$_4$[$(H_3O)M(C_2O_4)_3$]C_5H_5N samples with M=Ga, Cr, and Fe. These frequencies are $F_\alpha\approx$38–50 T, $F_\beta\approx$86–98 T, $F_\gamma\approx$293–308 T, and $F_\delta\approx$345–353 T; the ranges cover the values observed in the different samples (see Table II). In addition, two other peaks, with frequencies $F'\approx$190–206 T and $F''\approx$236–248 T, were observed less consistently in the transforms. The peak at very low frequencies ($\lesssim$20 T) is an artifact of the subtraction of the background magnetoresistance; its position and amplitude depends on whether R_{bg} was approximated by a second or

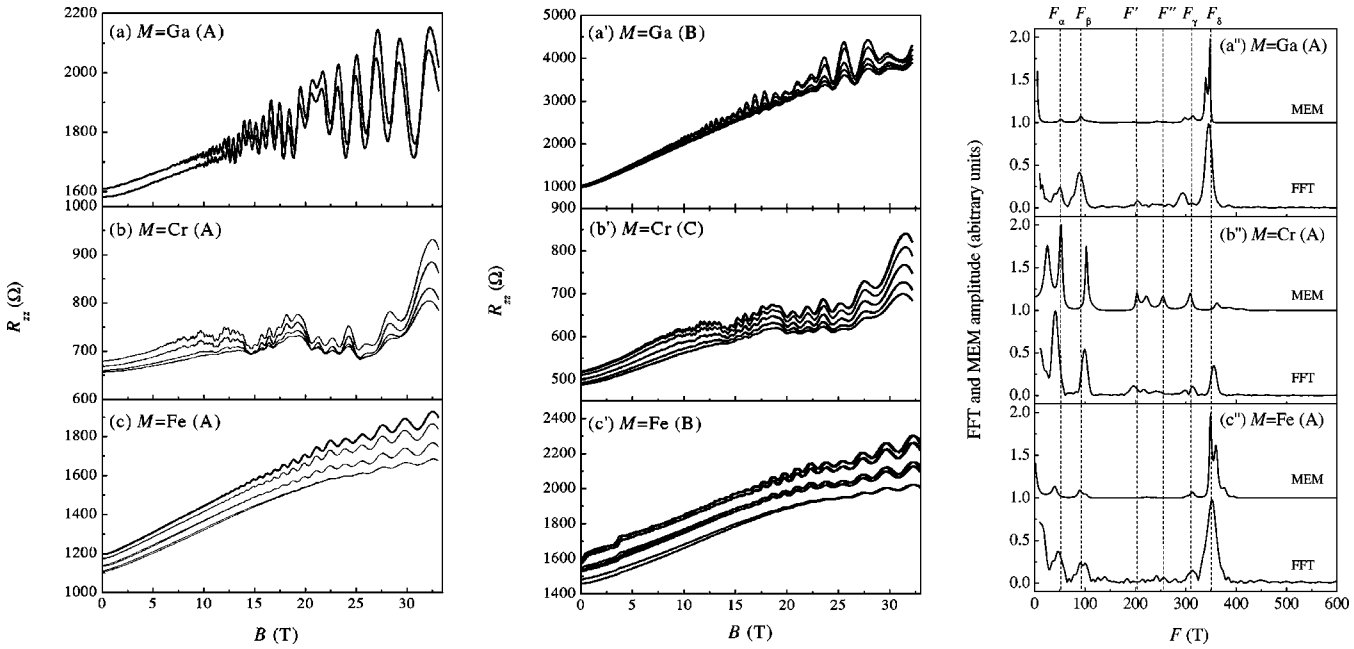

FIG. 4. Magnetic field dependence of the interplane resistance, R_{zz}, for β''-(BEDT-TTF)$_4$[$(H_3O)M(C_2O_4)_3$]C_5H_5N samples $M=$Ga [samples A (a) and B (a′)], $M=$Cr [samples A (b) and C (b′)] and $M=$Fe [samples A (c) and B (c′)], recorded between $T=0.5$–4.2 K. The right panel [(a″), (b″), and (c″)] corresponds to the maximum entropy method (top solid lines) and fast Fourier transform spectra (bottom solid lines) of the oscillatory component of the resistance, $[(R_{zz}-R_{bg})/R_{bg}$, where R_{bg} is a polynomial fit] over the field range 7–32 T; the transforms correspond to the data from the left panel at $T=0.5$ K. The dashed vertical lines indicate the approximate positions of the frequencies discussed in the text.

fourth-order polynomial in B. In some cases, the peak at frequency F_α is superimposed on the flank of this feature, making a precise determination of the frequency difficult.

Because of their dependence on temperature (see below), magnetic-field orientation (all frequencies vary as $1/\cos\theta$, where θ is the angle between the magnetic field and the normal to the quasi-two-dimensional planes[44]) and their consistent appearance in the transforms, we attribute the Shubnikov–de Haas frequencies F_α, F_β, F_γ and F_δ to the extremal orbits about four independent quasi-two-dimensional Fermi-surface pockets, which we label α, β, γ, and δ. As for the other peaks, we note that as $F'\approx 2F_\beta$, it is likely to be a second harmonic of the oscillations due to the β pocket.

The peak seen occasionally in the transforms at a frequency F'' seems likely to result from frequency-mixing effects and it can be constructed using a variety of recipes (for example, $F''\approx F_\alpha+2F_\beta$, $F''\approx F_\gamma-F_\alpha$, $F''\approx F_\delta-F_\beta$). Such frequency-mixing effects in quasi-two-dimensional metals are often attributable to the chemical potential becoming pinned to relatively sharp Landau levels over restricted regions of magnetic field [the so-called ''chemical potential oscillation effect'' (CPOE)],[45,46] which, in some cases, very complex mixed harmonics are generated.[47] Another possibility which can determine a difference frequency is the Stark quantum interference effect;[42] this represents ''interference'' of two semiclassical Fermi-surface orbits between which tunnelling can occur. However, the oscillations due to the Stark quantum interference effect are usually characterized by an apparent very light effective mass; that is, their amplitude varies more slowly with temperature than that of the oscillations due to the two ''parent'' orbits.[48] The fact that, when present, the oscillations at F'' are suppressed much more rapidly with increasing temperature than any of the possible parent frequencies suggests that CPOE is the more likely explanation.[49,51]

At this point, it is worth recalling that the band structure calculations predict only two Fermi-surface pockets, of equal area,[32] whereas the experimental data suggest four pockets. There are several potential reasons for this difference. First, whilst extended-Hückel calculations often give a reasonable qualitative description of the Fermi surfaces of many BEDT-TTF salts,[3] the β'' phases have proved problematic; slight differences in input parameters seem to result in differing predicted topologies [as in the case of β''-(BEDT-TTF)$_2$AuBr$_2$ (Ref. 50)]. Secondly, the band structure calculations are based on structural measurements carried out at relatively high temperatures;[22] contraction of the lattice could result in changes in the relative sizes of the various transfer integrals, leading to shifts in the bands with respect to the chemical potential. Finally, the presence of a series of pockets could be a consequence of a Fermi surface reconstruction determined by a possible charge-density wave at T_{MI} of the β''-(BEDT-TTF)$_4$[$(H_3O)M(C_2O_4)_3$]C_5H_5N salts. Similar Fermi-surface reconstructions have been suggested for other β'' salts, including β''-(BEDT-TTF)$_2$AuBr$_2$ (where a plethora of small Fermi surface pockets results),[50] β''-(BEDO-TTF)$_2$ReO$_4$H$_2$O (Ref. 33) and β''-(BEDT-TTF)$_2$SF$_5$CH$_2$CF$_2$SO$_3$, where it appears that the Fermi-surface nesting is more efficient.[52]

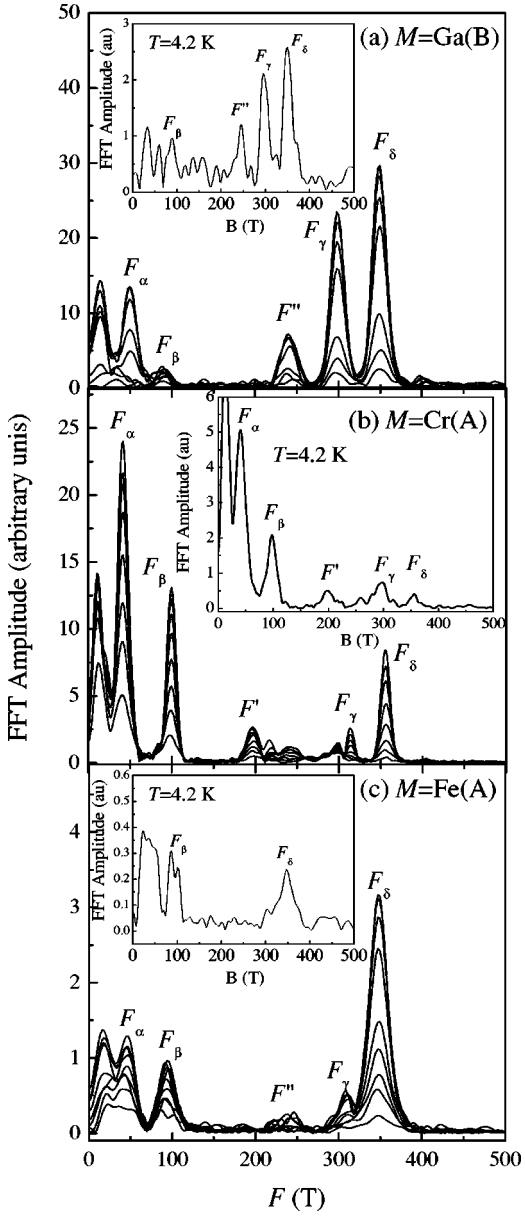

FIG. 5. Fast Fourier transforms of Shubnikov–de Haas oscillations for samples of β''-(BEDT-TTF)$_4$[$(H_3O)M(C_2O_4)_3$]C_5H_5N. (a) $M=$Ga (B), (b) $M=$Cr (A) and (c) $M=$Fe (A) recorded between $T=0.5$ K and $T=4.2$ K.

In spite of the larger number of Fermi-surface pockets observed experimentally, there are some similarities with the calculated Fermi surface. First, the largest experimental pocket, δ, is of a similar cross-sectional area ($\approx$8.5% of the Brillouin cross section) to the calculated pockets (8.1% of the Brillouin-zone cross section).[32] Secondly, as noted above, the β''-(BEDT-TTF)$_4$[$(H_3O)M(C_2O_4)_3$]Y salts are expected to be quasi-two-dimensional compensated semimetals in which the cross-sectional areas of the hole Fermi-surface pockets should sum to the same value as the total cross-sectional area of the electron Fermi-surface pockets. We note that $F_\alpha+F_\delta \approx F_\beta+F_\gamma$ to reasonable accuracy (Table II). This suggests that if α and δ are electron (hole) pockets, then β and γ will be hole (electron) like.

Although the Shubnikov–de Haas oscillation frequencies are generally similar for the three β''-(BEDT-TTF)$_4$[$(H_3O)M(C_2O_4)_3$]C_5H_5N salts, there are detail differences depending on the ion M. For example, the F_α frequency of the $M=$Cr salts is consistently lower than that of the $M=$Ga and Fe compounds. The appearance of the Shubnikov–de Haas oscillations is also affected by the M ion; the highest frequency oscillations (F_δ) dominate the spectra of the compounds with $M=$Ga and Fe, whereas that of the compounds with $M=$Cr is dominated by the low frequency, F_α (see Figs. 4 and 5). This may be related to relatively small differences in the scattering mechanisms, rather than some intrinsic effect of the Cr^{3+} ion. Examples of similar effects were observed in magnetoresistance data for the low-field, low-temperature phases of α-(BEDT-TTF)$_2$KHg(SCN)$_4$ and α-(BEDT-TTF)$_2$TlHg(SCN)$_4$.[53] The relative amplitudes of the various Shubnikov–de Haas oscillation series vary from sample to sample, and batch to batch, with some series being undetectable in what is presumed to be the lower-quality samples, whilst being relatively strong in other crystals (see Secs. 1 and 5 of Ref. 53 and references cited therein). A second example is β''-(BEDT-TTF)$_2$AuBr$_2$ for which comparison of the magnetic-quantum oscillation data from Refs. 50, 54–56 shows that the relative amplitudes of the lower and higher-frequency oscillation series varies considerably from sample to sample.

For completeness, we mention that the superconducting salts, $Y=C_6H_5NO_2$ with $M=$Ga and Cr and $Y=C_6H_5CN$ with $M=$Fe show only two frequencies, with the low frequency in the range 47–55 T and the high frequency in the range 190–238 T.[24]

B. Effective masses

A two-dimensional Lifshitz-Kosevich formula[57] has been used to extract the effective masses m^* of the various Fermi-surface pockets, where possible. The Fourier amplitude of each series of quantum oscillations is given by

$$A_{2D} \propto R_T R_D R_S, \tag{2}$$

where $R_T=X/\sinh(X)$ is the temperature damping term, $R_D=\exp(-X(T_D/T))$ is the Dingle term (T_D is the Dingle temperature) due to the broadening of the Landau levels caused by internal inhomogeneities and $X=14.694(T/B)(m^*/m_e)$.

The spin-splitting term $R_S=|\cos((\pi/2)[(g^*m^*/m_e)/\cos(\theta)])|$, where g^* is the effective g factor, is not considered here and it will be the subject of a future publication.[44]

The Fourier amplitudes obtained over a field window 7–32 T were fitted to the R_T term of Eq. (2) using around 8 different temperatures covering the range 0.5–4.2 K (for consistency, a polynomial of the same order was used to subtract the background magnetoresistance for each sample). Figure 6 shows typical amplitudes and corresponding fits for the F_δ series. All of the m^* values obtained for the different Fermi-surface pockets are listed in Table II.

To the limit of experimental error the effective masses for the γ and δ pockets of the three salts are close to the free-electron mass, m_e. Whilst such values are light compared to

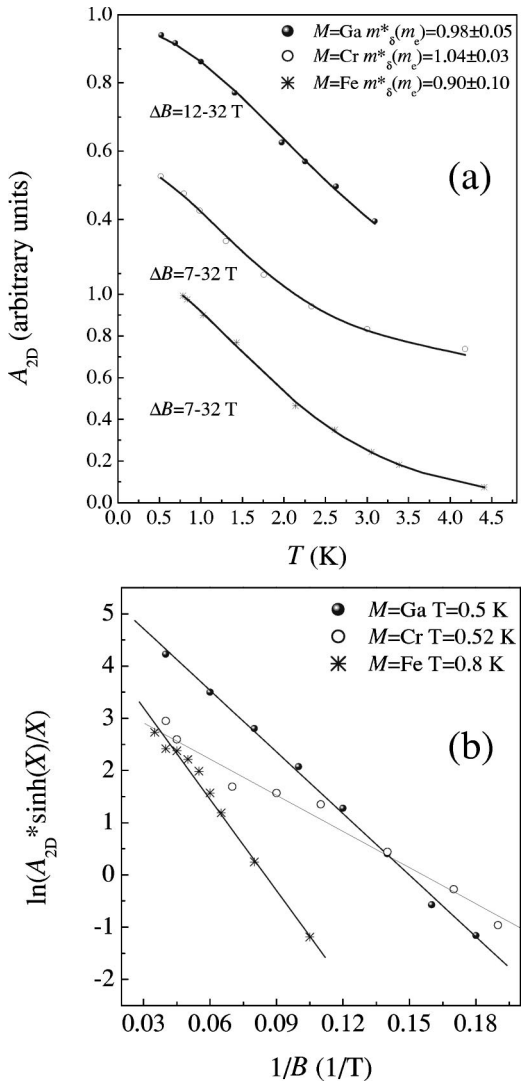

FIG. 6. (a) Temperature dependence of the Fourier amplitude of the F_δ frequency in β''-(BEDT-TTF)$_4$[$(H_3O)M(C_2O_4)_3$]C_5H_5N for different M. The solid line is a fit to the data (points) using the R_T term of Eq. (2) (solid line). The field window was $\Delta B = 7-32$ T for the samples with $M=$Cr (sample A) and $M=$Fe (sample A) and $\Delta B = 12-32$ T for the sample with $M=$Ga (sample A). Data for different M are offset for clarity. (b) The corresponding Dingle plots ($\ln[A_{2D}\sinh(X)/X]$ versus $1/B$, where $X = 14.695\ m^*T/B$) for the F_δ frequency at $T \approx 0.5$ K. The solid line is a linear fit to the data (points). The field windows overlapped by less than $\approx 30\%$.

the typical masses observed in β''-(BEDT-TTF)$_2SF_5CH_2CF_2SO_3$ (Ref. 52) or the κ- and α-phase BEDT-TTF salts,[42] they are not without precedent in charge-transfer salts.[33,34] The effective masses of the α pocket are somewhat smaller for the $M=$Cr and Fe salts ($m^* \approx m_e/2$) whereas in the case of the $M=$Ga salt, the α effective mass seems rather larger. Apart from this, there is yet no evidence that the magnetic moment on the $3d$ ions $M=$Cr and Fe has any effect on the effective masses. This is in contrast to the study on κ-(BETS)$_2$FeCl$_4$, where it was proposed that spin fluctuation effects enhanced the effective mass.[58] On the other hand, the effective mass in λ-(BETS)$_2$Fe$_x$Ga$_{1-x}$Cl$_4$ is not very much affected by the presence of the magnetic ions but it is much larger than that in our compounds [$\approx 4m_e$ (Ref. 30)].

C. Dingle temperatures

A further insight into the properties of our samples is given by the Dingle temperature, T_D, which can be used to parametrize the scattering rate,[20,41] the spatial potential fluctuations or a combination of the two.[9,20] The T_D values for the δ pocket are listed in Table II; typical fits are shown in Fig. 6(b). Note that T_D is consistently larger for the compounds with $M=$Fe ($T_D \approx 4$ K, corresponding to a scattering time of $\tau \approx 0.3$ ps) and is smaller for the salts with $M=$Cr ($T_D \approx 1.5$ K, corresponding to $\tau \approx 0.8$ ps). This difference is visible even in the raw data, with fewer oscillations being visible for the $M=$Fe salt. As both compounds contain magnetic ions some form of magnetic scattering (such as spin-disorder scattering[59]) may be excluded as the reason for these differences and the degree of nonmagnetic disorder present, determined by the anions and the solvent is more likely to be the determining factor.

Interestingly, there is no apparent correlation between the values of $R_{zz}(T)/R_{zz}(286\ \mathrm{K})$ (see Fig. 3) and the Dingle temperatures for each sample (Table II). For example, the sample with the largest $R_{zz}(T)/R_{zz}(286\ \mathrm{K})(\approx 7)$ ($M=$Cr, sample A) has a T_D which is a factor 2.2 smaller than that of the sample with the smallest $R_{zz}(T)/R_{zz}(286\ \mathrm{K})(\approx 0.5)$ ($M=$Fe, sample A). The Dingle temperatures extracted from Shubnikov–de Haas oscillations suggest that $M=$Cr, sample A is of higher quality, whereas $M=$Fe, sample A has the lower resistivity ratio. This strongly suggests that the samples are not of a uniform single phase at the lowest temperatures but their overall properties probably represent a mixture of metallic and insulating domains. Within this mixture, the metallic domains may well be of quite high quality, as evidenced by the observation of Shubnikov–de Haas oscillations with a reasonably small Dingle temperature.

Further support for such an idea is given by comparing the values of $R_{zz}(10\ \mathrm{K})/R_{zz}(286\ \mathrm{K}) \sim 0.5$–$7$ seen in Fig. 3 with $R_{zz}(10\ \mathrm{K})/R_{zz}(286\ \mathrm{K}) \sim 0.001$ obtained for the unambiguously metallic salt β-(BEDT-TTF)$_2$I$_3$.[60] This great disparity is an indication that a large fraction of the quasiparticles in the β''-(BEDT-TTF)$_4$[$(H_3O)M(C_2O_4)_3$]C_5H_5N salts that are mobile at room temperature do not contribute to the bulk conductivity at low temperatures. This loss of charge carriers is presumably related to the suggested density-wave transition at T_{MI} (which perhaps gaps part of the Fermi surface) and to the subsequent ''freezing out'' of further quasiparticles (suggested by the negative dR_{zz}/dT values seen for several of the samples as shown in Fig. 3) caused by disorder at lower temperatures.

In summary, it is most likely that the Dingle temperature gives a gauge of only the quality of the *metallic* regions of the samples, whereas the $R_{zz}(\mathrm{T})/R_{zz}(286\ \mathrm{K})$ values are indicative of the relative proportion of insulating *and* metallic domains within the crystals.

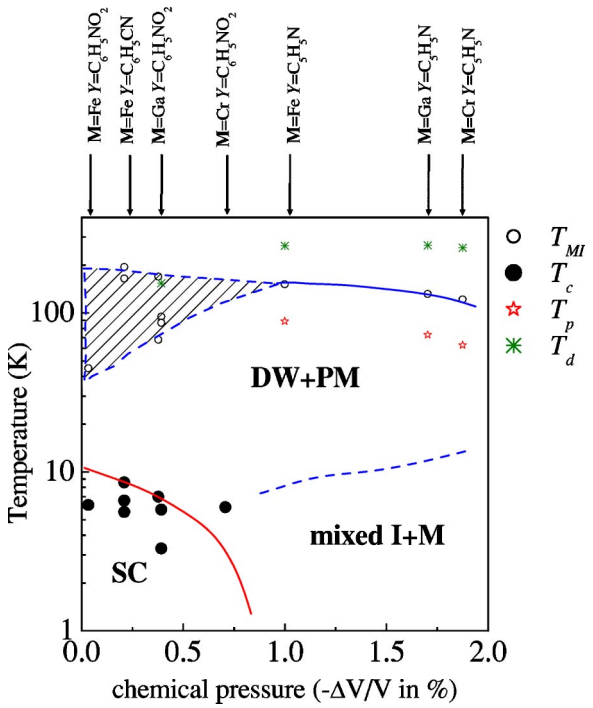

FIG. 7. Notional phase diagram of the β''-(BEDT-TTF)$_4$[$(H_3O)M(C_2O_4)_3$]Y salts, using data from the current paper and from Ref. 24. Solid circles correspond to the superconducting critical temperature, T_c; open circles represent the metal-insulator transition, T_{MI}. The other temperatures, T_p and T_d, are described in the text. Different phases are as follows: SC is superconducting, DW is density wave, M is metallic, PM is paramagnetic metallic and I is insulating phase. The solid and dashed lines are guides to the eye. The hatched region shows the distribution in the T_{MI} values for the superconducting samples determined by the differences in the cooling rate and samples quality.

V. DISCUSSION: PROPOSED PHASE DIAGRAM

In the previous sections we have described the transport properties of β''-(BEDT-TTF)$_4$[$(H_3O)M(C_2O_4)_3$]C_5H_5N salts exhibiting a metal-insulator transition at T_{MI} (probably associated with a density-wave state) and Shubnikov–de Haas oscillations at lower temperatures, indicative of a reasonably good metal. However, depending on the sample batch, the overall resistivity can be much greater than that at room temperature; the most likely explanation is that the sample consists of a mixture of metallic and insulating domains. The tendency for a particular region of the sample to remain metallic or become insulating may be linked to particular configurations of the anion and/or ethylene groups possible in the β''-(BEDT-TTF)$_4$[$(H_3O)M(C_2O_4)_3$]C_5H_5N salts (see Sec. III).

These findings are summarized in Fig. 7, which shows a notional phase diagram for all of the β''-(BEDT-TTF)$_4$[$(H_3O)M(C_2O_4)_3$]Y salts as a function of "chemical pressure" ($=-\Delta V/V$), i.e., the fractional difference in unit-cell volume of a particular salt from that of the $M=$Fe, $Y=C_6H_5NO_2$ compound, which has the largest unit cell. First, the superconductivity in the β''-(BEDT-TTF)$_4$[$(H_3O)M(C_2O_4)_3$]Y salts is suppressed by the reduction in volume of the unit cell. The suppression of superconductivity is accompanied by the increasingly "metallic" character evidenced by the increase in the number and size of Fermi-surface pockets observed (two for $Y=C_6H_5NO_2$, C_6H_5CN, four generally larger ones for $Y=C_5H_5N$). This trend is confirmed by hydrostatic pressure measurements of the superconducting β''-(BEDT-TTF)$_4$[(H_3O)Ga$(C_2O_4)_3$]Y salts, which showed that the superconductivity is destroyed and the number of Fermi-surface pockets increased by increasing pressure.[61] Secondly, the superconducting state may be surrounded by regions in which metallic and insulating behavior coexist in the "PM+DW" phase.

Although the work on β''-(BEDT-TTF)$_4$[$(H_3O)M(C_2O_4)_3$]Y salts is at an early stage, it is possible to note some qualitative similarities between Fig. 7 and the phase diagram of κ-(BEDT-TTF)$_2X$ (see Refs. 1, 10 and references therein).[65] Increasing pressure also results in more metallic behavior in the κ salts, as evidenced by the Shubnikov–de Haas frequencies. Moreover, the superconducting region in both β'' and κ salts is surrounded by nonuniform or mixed phases.[8]

The study of β''-(BEDT-TTF)$_4$[$(H_3O)M(C_2O_4)_3$]Y salts seems to emphasize the fact that very highly resistive samples and phenomena associated with quasiparticle localization (e.g., Anderson localization[62]) and/or disorder[63] coexist with effects normally associated with "good metals," such as Shubnikov–de Haas oscillations[64] and even superconductivity.[62] Furthermore, there is experimental evidence that the precursor to superconductivity may involve the coexistence of metallic and density-wave-like states, such as the case of β''-(BEDT-TTF)$_2SF_5CH_2CF_2SO_3$ (Ref. 52) or κ-(BEDT-TTF)$_2X$.[8] These phases may exist in distinct "domains" or regions of the sample, as suggested in the case of the κ-phase salts,[10] the behavior of a particular domain being determined by local structural arrangements.

Finally, recent theoretical work has emphasized the role of disorder in the suppression of superconductivity in BEDT-TTF salts. Often a measure of this disorder is derived from Shubnikov–de Haas–oscillation or cyclotron-resonance data.[20] The resistivity data indicate that disorder makes some regions of the samples prone to localization and these regions contribute little to the low-temperature conductivity. Other regions remain metallic and exhibit Shubnikov–de Haas oscillations, indicative of reasonably long scattering times and mean-free paths $\sim$300 Å and hence low disorder. This suggests that the Shubnikov–de Haas and cyclotron resonance data are only informative about the disorder in the metallic regions of a sample.

VI. SUMMARY

In conclusion we have studied the Fermi-surface topology of β''-(BEDT-TTF)$_4$[$(H_3O)M(C_2O_4)_3$]Y, with $M=$Ga, Cr, Fe and $Y=C_5H_5N$. All of the studied salts exhibit similar Shubnikov–de Haas–oscillation spectra, which we attribute to four quasi-two-dimensional Fermi-surface pockets. The cross-sectional areas of the pockets are in agreement with the expectations for a compensated semimetal, and the corresponding effective masses are $\sim m_e$, rather small compared

to those of other BEDT-TTF salts. Apart from the case of the smallest Fermi-surface pocket, varying the M ion seems to have little effect on the overall Fermi-surface topology or on the effective masses.

Despite the fact that all samples show quantum oscillations at low temperatures, indicative of Fermi liquid behavior, the sample and temperature dependence of the interlayer resistivity lead us to suggest that these systems are intrinsically inhomogeneous. It is possible that the intrinsic tendency to disorder in the anions and/or the ethylene groups of the BEDT-TTF molecules leads to phase separation of the samples into insulating and metallic states.

Based on the data in this paper, and those from Ref. 24, we have constructed a notional phase diagram for the β''-(BEDT-TTF)$_4$[$(H_3O)M(C_2O_4)_3$]Y salts which exhibits some similarities with that of the κ-(BEDT-TTF)$_2X$ superconductors.

ACKNOWLEDGMENTS

This work is supported by EPSRC (UK), the Royal Society (UK), INTAS (project number 01-2212) and by the US Department of Energy (DOE) under Grant No. LDRD-DR 20030084. Work at the National High Magnetic Field Laboratory is performed under the auspices of the National Science Foundation, the State of Florida and DOE. We are grateful to Professor E. Canadell for sending us the results of his band structure calculations. We thank Dr. N. Harrison and Dr. J. Lashley for fruitful discussions, and Dr. A.-K. Klehe and Dr. V. Laukhin for useful comments and access to their recent high-pressure data.

*Present address: Department of Material Science, Graduate School and Faculty of Science, Himeji Institute of Technology, Hyogo 678-1297, Japan.

†Present address: Department of Organic and Polymeric Materials, Tokyo Institute of Technology, Tokyo 152-8552, Japan.

[1] R.H. McKenzie, Science **278**, 820 (1997).

[2] K. Kanoda, Physica C **282-287**, 299 (1997).

[3] J. Singleton and C.H. Mielke, Contemp. Phys. **43**, 63 (2002).

[4] S. Lefebvre, P. Wzietek, S. Brown, C. Bourbonnais, D. Jerome, C. Meziere, M. Fourmigue, and P Batail, Phys. Rev. Lett. **85**, 5420 (2000).

[5] K. Miyagawa, A. Kawamoto, and K. Kanoda, Phys. Rev. Lett. **89**, 017003 (2002).

[6] H. Ito, G. Saito, and T. Ishiguro, J. Phys. Chem. Solids **62**, 109 (2001).

[7] P. Limelette, P. Wzietek, S. Florens, A. Georges, T.A. Costi, C. Pasquier, D. Jerome, C. Meziere, and P. Batail, cond-mat/0301478 (unpublished).

[8] T. Sasaki, N. Yoneyama, A. Matsuyama, and N. Kobayashi, Phys. Rev. B **65**, 060505 (2002).

[9] J. Müller, M. Lang, F. Steglich, J.A. Schlueter, A.M. Kini, and T. Sasaki, Phys. Rev. B **65**, 144521 (2002).

[10] J. Singleton, C.H. Mielke, W. Hayes, and J.A. Schlueter, J. Phys.: Condens. Matter **15**, L203 (2003).

[11] V.Z. Kresin and W.A. Little, *Organic Superconductivity* (Plenum, New York, 1990).

[12] H. Akutsu, K. Saito, and M. Sorai, Phys. Rev. B **61**, 4346 (2000).

[13] A. Sato, H. Akutsu, K. Saito, and M. Sorai, Synth. Met. **120**, 1035 (2001).

[14] M.A. Tanatar, T. Ishiguro, S. Kagoshima, N.D. Kushch, and E.B. Yagubskii, Phys. Rev. B **65**, 064516 (2002).

[15] M. Maksimuk, K. Yakushi, H. Taniguchi, K. Kanoda, and A. Kawamoto, cond-mat/0305680 (unpublished).

[16] B.H. Brandow, Philos. Mag. **83**, 2487 (2003).

[17] K. Kuroki, T. Kimura, R. Arita, Y. Tanaka, and Y. Matsuda, Phys. Rev. B **65**, 100516 (2002); H. Kondo, and T. Moriya, J. Phys.: Condens. Matter **11**, L363 (1999).

[18] J. Merino and R.H. McKenzie, Phys. Rev. Lett. **87**, 237002 (2001); M. Calandra, J. Merino, and R.H. McKenzie, Phys. Rev. B **66**, 195102 (2002).

[19] G. Varelogiannis, Phys. Rev. Lett. **88**, 117005 (2002).

[20] B.J. Powell and R.H. McKenzie, Phys. Rev. B **69**, 024519 (2004).

[21] M. Kurmoo, A.W. Graham, P. Day, S.J. Coles, M.B. Hursthouse, J. Caulfield, J. Singleton, F.L. Pratt, W. Hayes, L. Ducasse, and P.J. Guionneau, J. Am. Chem. Soc. **117**, 12 209 (1995).

[22] H. Akutsu, A. Akutsu-Sato, S.S. Turner, D. Le Pevelen, P. Day, V. Laukhin, A.-K. Klehe, J. Singleton, D.A. Tocher, M.R. Probert, and J.A.K. Howard, J. Am. Chem. Soc. **124**, 12 430 (2002).

[23] S.S. Turner, P. Day, K.M.A. Malik, M.B. Hursthouse, S.J. Teat, E.J. Maclean, L. Martin, and S.A. French, Inorg. Chem. **38**, 3543 (1999).

[24] A. Bangura *et al.* (unpublished); A.F. Bangura, A.I. Coldea, J. Singleton, A. Ardavan, A.K. Klehe, A. Akutsu-Sato, H. Akutsu, S.S. Turner, and P. Day, Synth. Met. **1-3**, 1313 (2003).

[25] L. Martin, S.S. Turner, P. Day, P. Guionneau, J.A.K. Howard, K.M.A. Malik, M.A. Hursthouse, M. Uruichi, and M. Yakushi, Inorg. Chem. **40**, 1363 (2001).

[26] S. Rashid, S.S. Turner, P. Day, J.A.K. Howard, P. Guionneau, E.J.L. McInnes, F.E. Mabbs, R.J.H. Clark, S. Firth, and T.J. Biggs, J. Mater. Chem. **11**, 2095 (2001).

[27] S. Uji, H. Shinagawa, T. Terashima, T. Yakabe, T. Terai, M. Tokumoto, A. Kobayashi, H. Tanaka, and H. Kobayashi, Nature (London) **410**, 908 (2001).

[28] L. Balicas, J.S. Brooks, K. Storr, S. Uji, M. Tokumoto, H. Tanaka, H. Kobayashi, A. Kobayashi, V. Barzykin, and L.P. Gorkov, Phys. Rev. Lett. **87**, 067002 (2001).

[29] V. Jaccarino and M. Peter, Phys. Rev. Lett. **9**, 290 (1962).

[30] S. Uji, C. Terakura, T. Terashima, T. Yakabe, Y. Terai, M. Tokumoto, A. Kobayashi, F. Sakai, H. Tanaka, and H. Kobayashi, Phys. Rev. B **65**, 113101 (2002).

[31] O. Cepas, R.H. McKenzie, and J. Merino, Phys. Rev. B **65**, 100502 (2002).

[32] T.G. Prokhorova, S.S. Khasanov, L.V. Zorina, L.I. Buravov, V.A. Tkacheva, A.A. Basakakov, R.B. Morgunov, M. Gerer, E. Canadell, R.P. Shibaeva, and E.B. Yagubskii, Adv. Funct. Mat. **13**, 403 (2003).

[33] S. Kahlich, D. Schweitzer, C. Rovira, J.A. Paradis, M.H. Whangbo, I. Heinen, H.J. Keller, B. Nuber, P. Belle, H. Brunner, and R.P. Shibaeva, Z. Phys. B: Condens. Matter **94**, 39 (1994).

[34] W. Lubczynski, S.V. Demishev, J. Singleton, J.M. Caulfield, L. du Croo de Jongh, C.J. Kepert, S.J. Blundell, W. Hayes, M. Kurmoo, and P. Day, J. Phys.: Condens. Matter **8**, 6005 (1996).

[35] J. Dumas and C. Schlenker, Int. J. Mod. Phys. B **7**, 4045 (1993).

[36] T. Sasaki, N. Toyota, M. Tokumoto, N. Kinoshita, and H. Anzai,

Solid State Commun. **75**, 93 (1990).
[37] V. Dobrosavljevic, D. Tanaskovic, and A.A. Pastor, cond-mat/0206529 (unpublished).
[38] An additional activated component must be introduced to reproduce the data for $M=$Cr sample A over the same temperature region.
[39] J.A. Schlueter, B.H. Ward, U. Geiser, H.H. Wang, A.M. Kini, J. Parakka, E. Morales, H.-J. Koo, M.-H. Whangbo, R.W. Winter, J. Mohtasham, and G.L. Gard, J. Mater. Chem. **11**, 2008 (2001).
[40] B.R. Jones, I. Olejniczak, J. Dong, J.M. Pigos, Z.T. Zhu, A.D. Garlach, J.L. Musfeldt, H.-J. Koo, M.-H. Whangbo, J.A. Schlueter, B.H. Ward, E. Morales, A.M. Kini, R.W. Winter, J. Mohtasham, and G.L. Gard, Chem. Mater. **12**, 2490 (2000).
[41] D. Shoenberg, *Magnetic Oscillations in Metals*, *Cambridge Monographs in Physics* (Cambridge University Press, Cambridge, England, 1984).
[42] J. Singleton, Rep. Prog. Phys. **63**, 1111 (2000).
[43] T.I. Sigfusson, K.P. Emilsson, and P. Mattocks, Phys. Rev. B **46**, 10 446 (1992).
[44] A.I. Coldea *et al.* (unpublished).
[45] See, e.g., E. Rzepniewski, R.S. Edwards, J. Singleton, A. Ardavan, and Y. Maeno, J. Phys.: Condens. Matter **14**, 3759 (2002) and references therein.
[46] N. Harrison, J. Caulfield, J. Singleton, P.H.P. Reinders, F. Herlach, W. Hayes, M. Kurmoo, and P. Day, J. Phys.: Condens. Matter **8**, 5415 (1996).
[47] J. Singleton, F. Nasir, and R.J. Nicholas, Proc. SPIE **659**, 99 (1986).
[48] M.V. Kartsovnik, G.Yu. Logvenov, T. Ishiguro, W. Biberacher, H. Anzai, and N.D. Kushch, Phys. Rev. Lett. **77**, 2530 (1996).
[49] Note that Shoenberg's mechanism for frequency-mixing effects due to the *oscillatory* magnetic field within the sample (Ref. 42) is not generally feasible in BEDT-TTF salts, because the low quasiparticle density results in a rather small oscillatory magnetization (Ref. 50). In this context, the *M* ion is also unimportant; our compounds do not show any long range magnetic order down to 0.5 K (Ref. 51).
[50] A.A. House, N. Harrison, S.J. Blundell, I. Deckers, J. Singleton, F. Herlach, W. Hayes, J.A.A.J. Perenboom, M. Kurmoo, and P. Day, Phys. Rev. B **53**, 9127 (1996).
[51] A.I. Coldea *et al.*, J. Magn. Magn. Mater. (to be published).
[52] M.-S. Nam, A. Ardavan, J.A. Symington, J. Singleton, N. Harrison, C.H. Mielke, J.A. Schlueter, R.W. Winter, and G.L. Gard, Phys. Rev. Lett. **87**, 117001 (2001).
[53] N. Harrison, E. Rzepniewski, J. Singleton, P.J. Gee, M.M. Honold, P. Day, and M. Kurmoo, J. Phys.: Condens. Matter **11**, 7227 (1999).
[54] M. Doporto, J. Singleton, F.L. Pratt, J. Caulfield, W. Hayes, J.A.A.J. Perenboom, I. Deckers, G. Pitsi, M. Kurmoo, and P. Day, Phys. Rev. B **49**, 3934 (1994).
[55] S. Uji, H. Aoki, M. Tokumoto, A. Ugawa, and K. Yakushi, Physica B **194**, 1307 (1994).
[56] M. Tokumoto, A.G. Swanson, J.S. Brooks, C.C. Agosta, S.T. Hannahs, N. Kinoshita, H. Anzai, M. Tamura, H. Tajima, N. Kuroda, A. Ugawa, and K. Yakushi, Physica B **184**, 508 (1993).
[57] N. Harrison, R. Bogaerts, P.H.P. Reinders, J. Singleton, S.J. Blundell, and F. Herlach, Phys. Rev. B **54**, 9977 (1996); N. Harrison, A. House, I. Deckers, J. Caulfield, J. Singleton, F. Herlach, W. Hayes, M. Kurmoo, and P. Day, *ibid.* **52**, 5584 (1995).
[58] N. Harrison, C.H. Mielke, D.G. Rickel, L.K. Montgomery, C. Gerst, and J.D. Thompson, Phys. Rev. B **57**, 8751 (1998).
[59] Y. Shapira, S. Foner, and N.F. Oliveira, Phys. Rev. B **10**, 4765 (1974).
[60] M. Tokumoto, I. Nishiyama, K. Murata, H. Anzai, T. Ishiguro, and G. Saito, Physica B & C **143**, 372 (1986).
[61] V. Laukhin and A.-K. Klehe (private communication).
[62] P. Goddard, S.W. Tozer, J. Singleton, A. Ardavan, A. Abate, and M. Kurmoo, J. Phys.: Condens. Matter **14**, 7345 (2002).
[63] I. Olejniczak, J.L. Musfeldt, G.C. Papavassiliou, and G.A. Mousdis, Phys. Rev. B **62**, 15 634 (2000).
[64] K. Storr, L. Balicas, J.S. Brooks, D. Graf, and G.C. Papavassiliou, Phys. Rev. B **64**, 045107 (2001).
[65] For instance there are no β'' compounds available with a large enough unit cell to check whether the low-pressure, low-temperature state from which superconductivity emerges is a Mott insulator, as in the case in the κ-phase salts.